Journal of Chromatography Open 8 (2025) 100233

Contents lists available at ScienceDirect

Journal of Chromatography Open

journal homepage: www.elsevier.com/locate/jcoa

Cutaneous volatile and semi-volatile organic compounds as markers of malaria-infection by wearable samplers and two-dimensional gas chromatography—time-of-flight-mass spectrometry

Daniel T. Pretorius [a], Egmont R. Rohwer [a,b], Yvette Naudé [a,b,*]

[a] Department of Chemistry, Faculty of Natural and Agricultural Sciences, University of Pretoria Lynnwood Rd, Hatfield 0028, Pretoria, Gauteng, South Africa
[b] University of Pretoria Institute for Sustainable Malaria Control (UP ISMC), South Africa

ARTICLE INFO

Keywords:
Human cutaneous volatiles
Plasmodium-infection differential marker
Malaria
Wearable sampling band
GCxGC-TOFMS

ABSTRACT

Malaria has been found to alter normal cutaneous volatile organic compound (VOC) profiles, suggesting their potential application as markers of *Plasmodium* infection. The cutaneous VOCs and semi-VOCs (SVOCs) of malaria-negative and -positive individuals, who visited two local clinics in the Vhembe district of Limpopo Province, South Africa, were extracted into wearable silicone rubber (polydimethyl siloxane [PDMS]) sampling bands adhered to the surface of the epidermis. After sampling of epidermal VOCs from participants the samplers were analysed by thermal desorption-comprehensive two-dimensional gas chromatography-time-of-flight-mass spectrometry (TD-GC × GC-TOFMS). Individual cutaneous VOCs and SVOCs profiles were constructed from these complex chromatographic profiles in order to identify potential signatures of *Plasmodium* infection. Fatty acid compounds associated with rancid malodour, and previously reported as mosquito attractants, were found at an overall greater abundance in chemical profiles of malaria-positive cases. A targeted analysis was performed for compounds previously reported to be associated with *Plasmodium* infection, viz., heptanal, (E)-2-octenal, 2-octanone, octanal, nonanal and (E)-2-decenal. The linearity (R^2) range was 0.93–0.99 for a matrix matched (simulated cutaneous sampling) calibration range of 2.5–60 ng. Limits of detection (LOD) ranged from 0.4 pg (2-octanone) to 6.3 pg ((E)-2-octenal), whilst limits of quantification (LOQ) ranged from 1.4 pg to 21.1 pg. The mean percentage recoveries ($n = 2$) ranged from 77.8 % ((E)-2-decenal) to 118.9 % (2-octanone). The percentage relative standard deviations (%RSDs; $n = 2$) ranged from < 1 % for 2-octanone, octanal and nonanal to 27.1 % for (E)-2-octenal. We found that this particular suite of compounds, previously reported as indicators of malaria, was in fact non-specific for *Plasmodium* infection when compared to control subjects with comorbidities. A previously unreported (in a malaria-infection context) compound, (E)-2-octen-1-ol, correlated with malaria-positive participants, but was also observed for two malaria-negative participants, which could indicate latent malaria. In chronic cases, *Plasmodium vivax* can occur in reservoirs outside of the bloodstream, and thus blood-based diagnostic tests can miss latent infection. A key advantage of the epidermal sampler over blood tests is that the former collects whole-body organic compounds, and is therefore not limited to blood-borne markers of infection. As such it appears to be feasible for future investigations.

1. Introduction

Malaria is a potentially fatal disease if not diagnosed and treated swiftly. The World Health Organisation (WHO) estimated a global total of 263 million cases of malaria in 2023, of which the majority occurred in Africa. Mortalities were estimated at 597 000 worldwide [1]. Mosquitoes of the genus *Anopheles* are the vectors of the malaria-causing *Plasmodium* parasite. Though there are over 100 known *Plasmodium* species, only four are known to infect humans: *Plasmodium falciparum, P. vivax, P. malariae* and *P. ovale* [2]. The African malaria female mosquito *Anopheles gambiae* is a chief vector of malaria throughout sub-Saharan Africa [3] with the majority of cases in Africa caused by *P. falciparum* [2].

Since conventional malaria testing methods involve invasive blood-draws, it is worth investigating alternative and less intrusive diagnostic procedures that utilise more readily available biofluids such as

* Corresponding author.
E-mail address: yvette.naude@up.ac.za (Y. Naudé).

https://doi.org/10.1016/j.jcoa.2025.100233
Received 24 April 2025; Received in revised form 9 June 2025; Accepted 11 June 2025
Available online 12 June 2025

exhaled breath [4]. Schaber et al. reported that malaria infection could alter metabolites in the breath of patients [5]. Volatile organic compounds (VOCs) in the breath collected from children with and without uncomplicated *P. falciparum* malaria were analysed by thermal desorption-comprehensive two-dimensional gas chromatography-time-of-flight-mass spectrometry (TD-GC × GC-TOFMS) [5]. The authors reported a suite of six compounds (previously found in the breath of healthy individuals [6]), that correlate with *Plasmodium* infection status: methyl undecane, dimethyl decane, trimethyl hexane, nonanal, isoprene, and tridecane [5].

Since there is a correlation between chemicals originating from the human epidermis and exhaled breath, the sampling of human epidermal emanations presents an attractive substitute, especially considering that the latter is considered to be a more infectious matrix, e.g. in the presence of tuberculosis (TB), a common comorbidity [7]. Cutaneous VOCs emitted from human skin may function as kairomones to *Anopheles* [3]. Also, malaria has been found to alter normal cutaneous VOC profiles [8, 9–12], suggesting their potential application as markers of *Plasmodium* infection. These Plasmodium-induced VOCs can be collected and analysed by gas chromatography-mass spectrometry *via* thermal desorption of samplers or injection of solvent extracts. The collection of surface cutaneous chemicals involves gauze, glass beads, polymer rods (PowerSorb®), socks, PTFE sleeves or bags, cellulose bags, or a whole-body headspace collection chamber [8,13,14–16]. These extraction techniques, however, are inconvenient, restrictive, or require non-wearable equipment such as pumps [7].

As an advanced separation technique, GCxGC is recognised as the gold standard in analysing complex mixtures [17–21]. It has evolved beyond conventional applications—such as environmental, petrochemical, and odourant analysis—to find use in metabolomics, where it can be used to tackle emerging challenges in untargeted analysis [22–24], for disease marker discovery, of complex samples such as exhaled breath [5,25,26].

Previously we have demonstrated that in-house prepared, non-invasive, wearable silicone rubber bands (PDMS) attached to the epidermis were well suited to the identification of differential markers in the context of tuberculosis diagnosis, as well as to the study of the attractiveness of different individuals to mosquitos [27–30]. They thus offer potential in the detection of compounds indicative of malaria-infection. Unlike exhaled breath, the silicone rubber band containing trapped compounds is not regarded as biological material. Here, we investigate the feasibility of the human epidermis as a safer biological medium for the detection of malaria-associated compounds with TD-GCxGC-TOFMS.

2. Methods and materials

2.1. Ethical considerations

The recruitment, testing and sampling protocol in this study were approved by the ethics committees of the faculties of the Natural and Agricultural Sciences (reference: NAS036/2019) and Health Sciences (reference 606/2019) of the University of Pretoria, with a validity of one year (2020). Permission to conduct the study in the government clinics of Masisi and Madimbo was granted by the Limpopo Provincial Department of Health (reference LP-202,002–014), as well as by signed consent from the Head Sisters of the respective clinics.

2.2. Study location, participant recruitment and sample population

The recruitment, testing and sampling of participants was conducted in two daytime government clinics, Masisi and Madimbo, in the Vhembe district of the Limpopo Province of South Africa, in March 2020. Patients visiting the respective clinics (with malaria-like symptoms or other ailments) were enrolled in the study as participants, and provided signed and informed consent to their participation. The pilot study cohort consisted of malaria-positive and malaria-negative participants, male and female (Table S1). Prior to testing, all participants filled in a questionnaire pertaining to aspects of general lifestyle and health (Table S2). A total of 25 participants were included in the study, of which three participants tested positive for malaria by microscope assay of peripheral blood smears (Ampath Laboratories, Pretoria, South Africa) and/or by an onsite Rapid Diagnostic Test (RDT; U-Test Malaria, Humor Diagnostica, Hermanstad, South Africa). Replicate cutaneous VOCs and SVOCs samples were obtained from each participant, giving a total sample size of 52 measurements. Originally, a larger sample size (50–80) was to be obtained, however due to the outbreak of the SARS-CoV2 virus, responsible for the COVID-19 pandemic, and the national lockdown that was implemented on the 27th of March 2020, further recruitment, testing and sampling were discontinued.

2.3. Sorptive sampling of cutaneous VOCs and SVOCs

The in-house developed wearable sampling bands [27] were prepared by cutting medical-grade silicone elastomer tubing (0.3 mm ID × 0.6 mm OD; SIL-TEK®, Technical Products Inc., Georgia, USA) into lengths of 10 cm which were joined end-to-end with a 1 cm length of uncoated capillary column (0.25 mm ID; SGE Analytical Science, Separation Scientific (Pty), Roodepoort, South Africa). Each band had an average mass of 300–350 mg. Prior to use, the bands were cleaned and conditioned: the loops were sonicated three times in a 1:1 *v/v* methanol: acetone solution for five minutes, and were then inserted individually into thermal desorption tubes (17.8 cm length x 4 mm ID x 6 mm OD) and conditioned under hydrogen gas (100 mL/min) at 280 °C, for over twelve hours, using an off-line Gerstel™ thermal desorption (TDS) unit (Chemetrix, Midrand, South Africa) [31].

Sorptive sampling of the epidermis was done by the first author – a non-medical professional. The inner side of the dominant wrist of each participant was daubed with commercial isopropanol swabs to wash the skin of contaminants. Triplicate PDMS sampling bands were placed side-by-side on the same area of the inner wrist, and then covered and secured with aluminised Mylar® film (5 cm × 11 cm; Hydroponic, South Africa; previously sonicated in a 1:1 v/v methanol:acetone solution for five minutes, and cleaned with an isopropanol swab prior to use) and hypoallergenic 3 M Micropore ™ surgical tape (120 mm L x 72 mm W; Dis-chem, Pretoria, South Africa) (Fig. 1). The purpose of the Mylar® film was to shield the sampling bands from the atmosphere during the sampling period. Participants were free to move around while the sampling bands were attached to their wrist. After 30 min, the surgical paper tape and Mylar® film were removed, the sampling bands collected, individually wrapped in heavy duty aluminium foil and stored

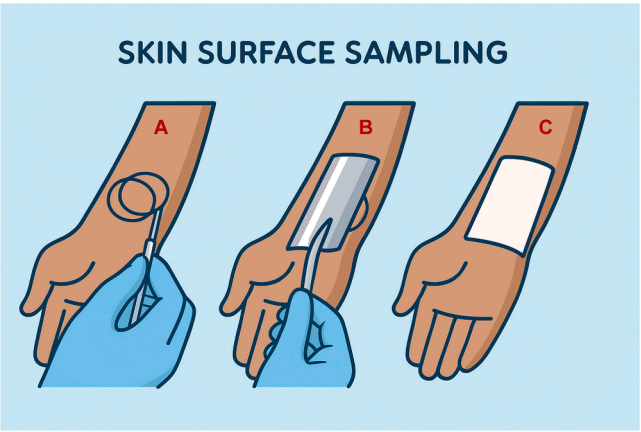

Fig. 1. Cutaneous VOCs and SVOCs sampling. (A) positioning of silicone rubber band samplers on the inner arm, (B) Mylar® cover, (C) hypoallergenic Micropore™ paper tape covering.

in a glass vial (labelled according to participant number and replicate number). These vials were kept in a cooler box and subsequently stored, upon return to the laboratory, in a freezer at −18 °C prior to analysis, which took place in November to December 2020.

2.4. Analytical standards

A solution of *n*-alkanes (C_8—C_{28}) used for the calculation of linear retention indices of reported analytes was purchased from Merck, South Africa. Analytical standards of heptanal (≥95 %), octanal (≥95 %), nonanal (≥99.5 %), trans-2-octenal (94 %), trans-2-decenal (≥95 %), and 2-octanone (≥99.5 %) were purchased from Sigma-Aldrich (Pty) Ltd., Kempton Park, South Africa, and were used for quantification and confirmation of the presence of these target analytes. These compounds have previously been reported in the literature on malarial volatile emissions [13]. A working solution (*n*-hexane, Merck, South Africa) containing 1 μg/mL of each target standard was prepared. Duplicate sampling bands were spiked, respectively, with 2.5, 5, 10, 15, 20, 40 and 60 ng of the working target standard solution. Each band was placed on a strip of Mylar wiped clean with a commercial isopropanol swab. The requisite volume of working target standard solution was applied to the surface of the mylar strip, adjacent to each band, and the mylar strip was folded over and wrapped closed with surgical micropore tape. The mylar/micropore tape package containing the band with spiked targeted standards was placed in a Schott glass bottle submerged in a water bath at 31 °C (to approximate epidermal surface temperature) for 30 min. After extraction each spiked band was wrapped in heavy duty aluminium foil and stored at −18 °C in a glass vial prior to analysis.

2.5. TD-GC × GC-TOFMS

Instrumental analysis was performed on a LECO© Pegasus 4D GC × GC-TOFMS fitted with a Gerstel™ TDS unit as an inlet, an Agilent© 7890 chromatograph and a dual quad-jet cryogenic modulator (LECO®, Kempton Park, South Africa), operated by ChromaTOF® software (version 4.51.6.0, optimised for Pegasus®). The hot jets were operated with synthetic air and the cold jets were operated with nitrogen gas (NM3OLA ML nitrogen gas generator, Peak Scientific, South Africa) cooled with liquid nitrogen (Afrox, South Africa). The primary (1D) capillary column was a Rxi-5MS of length 30 m x 250 μm ID x 0.25 μm film thickness; the secondary (2D) column was a Rxi-17SilMS mid-polar capillary column of length 0.760 m x 250 μm ID x 0.25 μm film thickness (Restek, USA).

Thermal desorption of the compounds from the PDMS sampling bands was performed with a Gerstel™ thermal desorption unit (TDS 3, Chemetrix, Midrand, South Africa), with the bands inserted into a glass thermal desorption tube. The heat of desorption was from 30 °C (held for 3 min) to 280 °C (held for 10 min) at 60 °C/min, with a flow rate of 100 mL/min at a vent pressure of 10 psi of helium (ultra-high purity grade; Afrox, Gauteng, South Africa). The TDS transfer line temperature was maintained at 350 °C. Cryogenic focussing of the desorbed compounds occurred at −100 °C, using liquid nitrogen (Afrox, Gauteng, South Africa) in a cooled injection system (Gerstel™ CIS 4) with an empty, baffled and deactivated glass liner. The thermally desorbed compounds were introduced into the inlet *via* a splitless injection (purge flow of 30 mL/min after 90 s, solvent vent mode) by heating the CIS from −100 °C, at 10 °C/s, to 250 °C (and held for the duration of the GC run). The carrier gas (ultra-high purity grade helium [Afrox, Gauteng, South Africa]) flow-rate was constant at 1.4 mL/min.

The initial temperature for the primary oven was held at 40 °C for 1.5 min, and ramped to 300 °C at a rate of 10 °C/min, with a hold time at this temperature of 8 min. The total run time was 35.5 min. The temperature programme rates for the secondary oven and the modulator were the same as that of the primary oven, but offset by +5 °C and +15 °C respectively. The transfer line to the TOFMS was maintained at a temperature of 300 °C. The modulation period was 3 s, with a hot pulse time of 0.8 s and a cool time between stages of 0.7 s.

The TOFMS was operated at an acquisition rate of 100 spectra/second over a mass range of 35–500 Daltons. The ionisation energy was 70 eV in the electron impact ionisation mode (EI+), the voltage of the detector was 1650 V, and the temperature of the ion source was 230 °C.

2.6. Data acquisition and processing

ChromaTOF® software (version 4.51.6.0, optimised for Pegasus®) was used for data acquisition and the VLOOKUP function of Microsoft® Excel® (version 16.0.14228.20204) for chromatographic peak alignment. A S/N threshold of 100 was set, and deviations in retention time were bound within the modulation period (3 s) for 1D peaks and 0.1 s for 2D peaks. Peak annotation was achieved by comparison of experimental mass spectra with reference spectra of the National Institute of Standards and Technology (NIST) library (version 2.2), with the minimum similarity threshold for a match set at 75 %. In addition, experimental linear retention indices (LRIs) were compared to literature LRIs in order to increase the level of confidence of peak annotation for untargeted analysis (Table 1). LRIs of reported analyte compounds were calculated using the method of the linear temperature programmed retention index, as developed by Van den Dool and Kratz [32]. Compounds having a match of within ± 35 RI units, or better (the majority), are reported. For targeted analysis, certified analytical standards were analysed. Targeted analytes were confirmed by retention time and mass spectral matching of standards to those present in samples.

2.7. Data analysis

Contaminant compounds were removed from the data set, including siloxanes, halogens, boronic compounds and metallic complexes. Blank correction, using duplicate-averaged blank PDMS sampling bands (i.e. which did not come into contact with skin), was performed for each sample replicate, resulting in a dataset ($N = 52$) of 3 166 compounds retained. R© computational and statistical software (version 1.3.959) with the Classification and Regression Training (caret) package (version 6.0–86) was used to construct models of the data (with cross-validation), to make class-based classification predictions, and to perform feature selection using three machine-learning algorithms: an Elastic-Net regression, Random Forest and Support-Vector Machine [33,34]. For this purpose, the data set was randomly shuffled and split with a 0.5 ratio into testing and training sets. Due to the paucity of malaria-positive samples obtained, replicates were treated individually in order to obtain a larger sample size for the train-test split. Chromatographic peak areas were normalised (centred and scaled) in terms of the peak area mean of each variable. A pared dataset of 1 128 variables were obtained after the removal of near-zero variance predictors. Normalised peak area values of the top variables were visualised as a heatmap, using the heatmap.2 function in the gplots package (version 3.1.3).

3. Results and discussion

3.1. Determination of malaria-infection status

The malaria-status was determined for each participant using the rapid diagnostic test (RDT) and microscopy. Of the twenty-five participants included, three showed at least one positive assay. The first (#4 female) tested positive by RDT for either *Plasmodium vivax (P. vivax), P. malariae* or *P. ovale*, but tested negative by microscopy. The second (#17 male) tested positive for *P. falciparum* by RDT and microscopic analysis, and had been infected with malaria three times previously. The third participant (#18 female) tested positive for *P. falciparum* by RDT, but tested negative by microscopy. This participant had also been infected with malaria on three previous occasions. The prolonged storage of the blood smears during the 2020 national lockdown period may have compromised the quality of the microscopy smears, resulting in false-

Table 1
Selected untargeted features obtained with Elastic-Net, Random Forest and Support-Vector Machine.

Compound name	CAS number	Molecular formula	Chemical class	MW (Da)	RI_{EXP} nonpolar	RI_{LIT} nonpolar (NIST)	MS similarity match
2-Octen-1-ol, (E)- (*trans*-2-octenol)	18409-17-1	C8H16O	Unsaturated alcohol	128	1040	1055; 1052	750–825
***n*-Decanoic acid**	334–48–5	C10H20O2	Saturated fatty acid	172	1361	1350;1373	752–934
Dodecanoic acid	143–07–7	C12H24O2	Saturated fatty acid	200	1561	1556;1568	762–937
Pentadecanoic acid	1002–84–2	C15H30O2	Saturated fatty acid	242	1827	1848	762–900
9-Hexadecenoic acid	2091–29–4	C16H30O2	Unsaturated fatty acid	254	1960	1976	751–774
2-Hexenoic acid, 3,4,4-trimethyl-5-oxo-, (Z)-	14919-56-3	C9H14O3	Keto acid	170	1247	Not available	752–754
2-Methylbutanoic anhydride	1468–39–9	C10H18O3	Acid anhydride	186	1185	1190	755–856
Isothiazole	288–16–4	C3H3NS	Azole	85	<800	743	768–775
Benzoic acid, 2-hydroxy-, pentyl ester	2050–08–0	C12H16O3	Benzoic acid ester	208	1618	1574; 1579	750–955
Formic acid, 2-propenyl ester	1838–59–1	C4H6O2	Unsaturated ester/ aldehyde	86	1015	1014	784–827
Propanoic acid, ethenyl ester	105–38–4	C5H8O2	Unsaturated ester/ aldehdyde	100	1057	1092	775–777
Naphthalene, 1,2,3,4-tetrahydro-1,4-dimethyl-	4175–54–6	C12H16	Naphthalene derivative	160	1275	1283; 1258	759–779
2,4-Nonadienal	6750–03–04	C9H14O	Unsaturated aldehyde	138	1210	1200	829–901
2,4-Decadienal, (E, E)-	25152-84-5	C10H16O	Unsaturated aldehyde	152	1262	1288; 1291	763–929
6-Methyl-3,5-heptadiene-2-one	1604–28–0	C8H12O	Unsaturated ketone	124	1058	1074	772–932
Undecane, 2,6-dimethyl-	17301-23-4	C13H28	Saturated hydrocarbon	184	1233	1210; 1218	752–904
Benzene, (2-methylpropyl)-	538–93–2	C10H14	Alkylbenzene	134	1001	1001; 997	752–913
Benzene, propyl-	103–65–1	C9H12	Alkylbenzene	120	929	944; 933	753–948
1H-Pyrazol-3-amine	1820–80–0	C3H5N3	Pyrazole derivative	83	1005	Not available	763–783
Isoamyl cyanide	542–54–1	C6H11N	Nitrile	97	823	814; 848	765–806
Butanamide, 3-methyl-	541–46–8	C5H11NO	Amide	101	1009	1018	757–850
2-Piperidinone	675–20–7	C5H9NO	Piperidine ketone	99	1147	1173	758–922
Pyridine, 3-ethyl-4-methyl-	529–21–5	C8H11N	Alkylpyridine	121	1017	1011	759–889

<800: Retention Index standard C_8—C_{28}. Literature Retention Indices from NIST14 library.

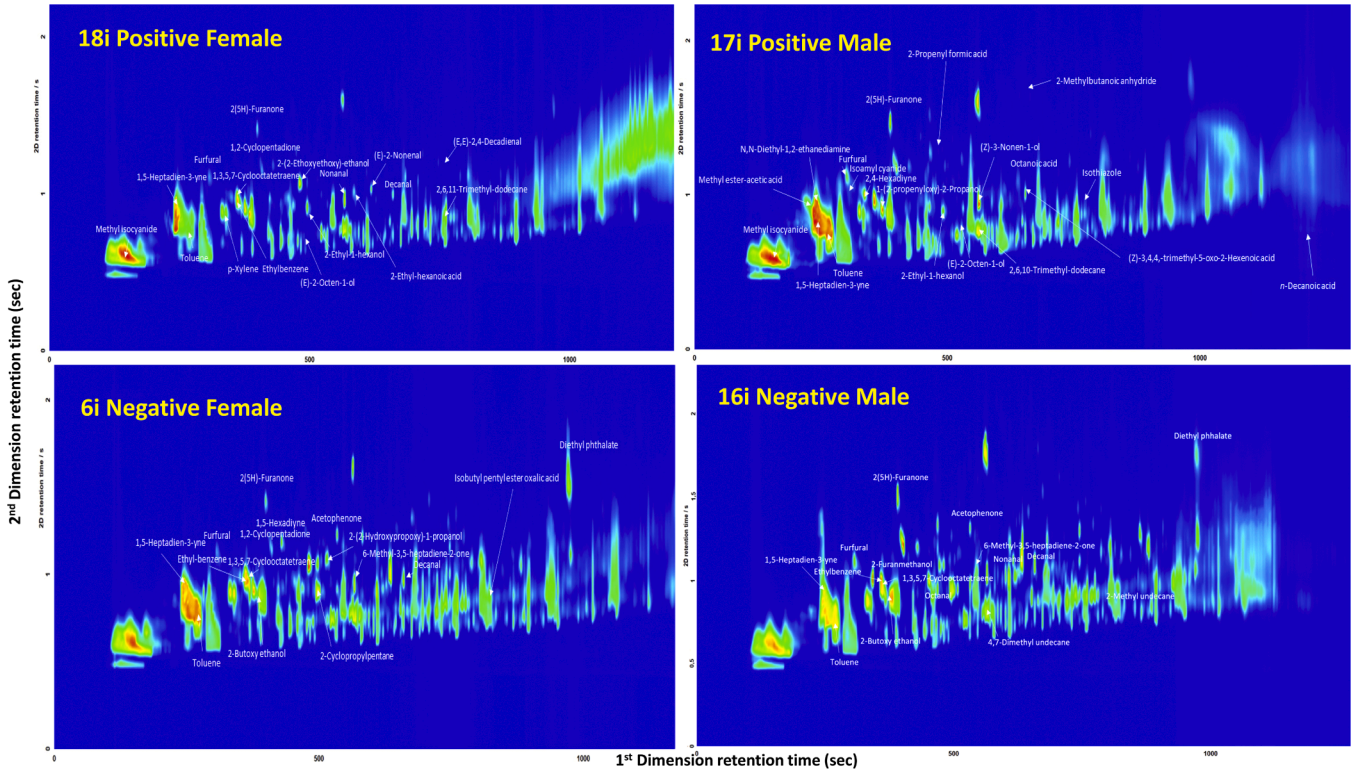

Fig. 2. TD-GCxGC-TOFMS contour plots (TICs) of surface epidermal emanations from (Top) female and male malaria-positive participants; (Bottom) female and male malaria-negative participants. Peaks of interest are in the 1D retention time region of 300–1000 s. Selected peaks are labelled either because they are top-ranking variables, are reported in literature [14] or because they are prominent peaks. Of note is that (E)-2-octen-1-ol is present in participants testing positive for *P. falciparum*, but absent for participants testing negative.

negatives for the RDT positive participants.

3.2. Untargeted analysis

The cutaneous chemical profiles, obtained by comprehensive GC × GC-TOFMS, are complex, showing dense peak distribution along the 2D separation space. A wide variety of organic species (C_3—C_{30}), of all major functional groups, are present on the surface of the epidermis (Fig. 2.).

The machine learning models do not have predictive value as to the infection status of the participants, due to the small sample set of positive subjects. Nevertheless, the top-ranking compounds resulting from feature selection (and used to construct the heatmap in Fig. 3) provide some information of potential significance regarding compounds potentially related to infection status. Table S3 lists the twenty top-ranking compounds for the three algorithms, as well as their scaled scores. A wide variety of compounds detected are selected as top features, including mid- to long-chain (C_{10}—C_{18}) saturated and unsaturated fatty acids, unsaturated alcohols; esters; aldehydes and ketones and alkylbenzenes. These are similar to compounds previously reported for *Plasmodium*-associated changes in human VOC profiles [13,14]. In addition, there are a number of nitrogenous compounds, including a pyrazole amine (1H-pyrazol-3-amine); a nitrile (isoamyl cyanide); an azole (isothiazole); amides and substituted pyridines. Compounds with a score of 100 are (E)-2-octen-1-ol, isoamyl cyanide and dicyclohexyl phthalate. The latter is an industrial product, and thus likely to be a contaminant. The C_8 unsaturated alcohol (E)-2-octen-1-ol is the only top differential feature for all three algorithms, with scaled scores of a 100 for Elastic-Net, 83 for Support-Vector Machine and 51 for Random Forest.

An unsaturated C_8 ketone, 6-methyl-3,5-heptadiene-2-one, listed for the support-vector machine, is similar to the C_8 ketone, 2-octanone, which has previously been reported to be associated with the presence of microscopic gametocytes [13]. The unsaturated C_9 aldehyde, 2,4-nonadienal is ranked highly by the support-vector machine, and is an unsaturated counterpart to nonanal, which has been found in elevated amounts in individuals infected with *Plasmodium* [13], but has also been found to be associated with underlying conditions and other diseases in malaria-free cases [14]. Two alkylbenzenes — (2-methylpropyl)-benzene and propyl-benzene — are also listed by the support-vector machine, and are similar to other alkylbenzenes that have been reported as compounds associated with malaria-infection, such as toluene, 1-ethyl-3-methyl- ethylbenzene and 1,2,4-trimethyl--benzene [14]. Notable peaks include the compounds (E)-2-octen-1-ol; 2-methylbutanoic anhydride; *n*-decanoic acid; isothiazole and isoamyl cyanide, and are indicated on the positive case #17 chromatogram (Fig. 2.). Retention indices (RIs) for selected ranked compounds are reported in Table 1, along with their unique CAS number and mass spectral similarity to the NIST mass spectral reference library.

3.3. Relative abundance of top-ranking compounds

The normalised peak area values of the top-ranking compounds are plotted as a heatmap in Fig. 3, representing their relative abundance across all replicate samples. Notably, the unsaturated alcohol, (E)-2-octen-1-ol, is present at significantly greater relative abundance for two of the malaria-positive cases. To the authors' knowledge (E)-2-octen-1-ol has not been previously reported in the context of *Plasmodium*-marker investigations. However, (E)-2-octen-1-ol has been evaluated as a chemical stimulus of the malaria mosquito *Anopheles sinensis* in the

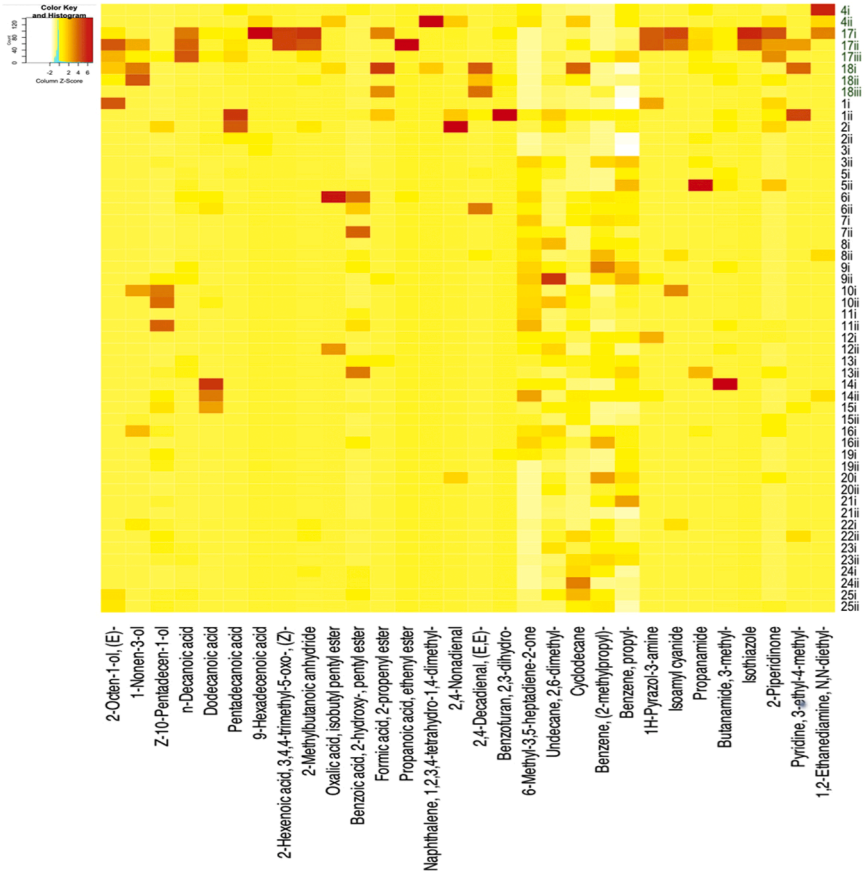

Fig. 3. Heatmap of sample-wise relative abundance (peak areas) of selected compounds from the human epidermis (Table 1). Malaria-positive participants (green, y-axis on the right); Malaria-negative participants (black, y-axis on the right). The colour intensity scale depicts the relative abundance Z-score.

context of host seeking and feeding behaviour [35] and has also been reported as a candidate attractant of the yellow fever mosquito *Aedes aegypti* [36]. This malaria- and yellow fever-mosquito attractant was present in both cases #17 (male) and #18 (female) testing positive for *P. falciparum*. Moreover, (E)-2-octen-1-ol was absent in 20 of 22 malaria-negative cases. However, it was also detected for malaria-negative cases #1 (female) and #25 (male). The latter case should be considered from the perspective that the participant visited the clinic because he had malaria-like symptoms. Indeed, *P. vivax* can occur outside the blood stream, other reservoirs being the spleen, bone marrow and skin. Thus, testing peripheral blood can miss chronic *Plasmodium* infections [37,38] which could point to potential latent malaria for these two cases. A significant advantage of the wearable epidermis sampler is that it is not limited to, or reliant on, the blood stream as a means of detection. This benefit could be exploited to identify latent cases (carriers of malaria that show no symptoms, but carry the parasite in the liver, spleen or bone marrow, and are generally not diagnosed by conventional blood tests). This is important for malaria eradication as asymptomatic carriers traversing borders are a significant reservoir of the *Plasmodium* parasite.

The following additional compounds are present at overall greater relative abundance (in terms of normalised peak area) in samples of positive cases: 9-hexadecenoic acid; *n*-decanoic acid; (Z)-3,4,4-trimethyl-5-oxo-2-hexenoic acid; 2-methylbutanoic anhydride; (E,E)-2,4-decadienal; propenyl ester formic acid; 1,2,3,4-tetrahydro-1,4-dimethylnaphthalene; N,N-diethyl-1,2-ethanediamine; isothiazole and isoamyl cyanide (Fig. 3). The collective presence of these compounds could potentially indicate *Plasmodium* infection. Compounds of a higher carbon number than C_{10}—C_{12} are less volatile, however, they may still potentially act as kairomones to Anopheline vectors that determine, at a proximal distance to the host, whether or not the mosquito will initiate landing and blood-feeding [39]. Notably, the compounds *n*-decanoic acid and 9-hexadecenoic acid (present at a comparatively higher relative abundance in malaria-positive patient #17 than in the negative participants) are carboxylic acids with rancid odours reminiscent of foot malodour, a scent profile which has been found to enhance host attraction to female Anopheline vectors [40,41]. In addition, 2-methylbutanoic anhydride (also present at greater relative abundance in positive case #17) is the anhydride of 2-methylbutanoic acid, which is an isomer of 3-methylbutanoic acid (isovaleric acid)— a known component of foot malodour [42]. The presence of these compounds may thus be associated with enhanced vector attraction in relation to malaria-infection status, and could thus also be potential signatures of malaria-infection.

In spite of a limited sample size of positive cases, these preliminary results support the feasibility of using the epidermis as an alternative biological medium for the detection of active and latent malaria, and as such a follow-up study incorporating a larger cohort is justified.

3.4. Targeted analysis

A targeted analysis for six compounds previously reported to be associated with *Plasmodium* infection was performed using analytical standards (Section 2.4). These compounds include heptanal, (E)-2-octenal, 2-octanone, octanal, nonanal and (E)-2-decenal [13]. Masses (ng) of these compounds present on the PDMS bands, as worn by the malaria-positive and malaria-negative participants, were calculated by linear regression analysis, and the results are summarised in Table S4. Limits of detection (LOD) ranged from 0.4 pg (2-Octanone) to 6.3 pg ((E)-2-Octenal) and limits of quantification (LOQ) ranged from 1.4 pg to 21.1 pg for the same compounds. The mean percentage recoveries ($n = 2$) ranged from 77.8 % ((E)-2-decenal) to 118.9 % (2-octanone) at a spiking level of 10 ng (Section 2.4). The percentage relative standard deviations (%RSDs; $n = 2$) ranged from < 1 % for 2-octanone, octanal and nonanal to 27.1 % for (E)-2-octenal.

Five malaria-negative cases (#3, #6, #13, #24 and #25) were chosen randomly as controls. Overall, there is little difference between the malaria-positive and -negative cases in terms of the targeted quantified masses, although nonanal is found at a relatively higher mass (8.8–24.4 ng) for positive case #17. The study reporting this suite of compounds involved foot odour collected on socks from infected and healthy uninfected participants [13]. In contrast, our finding that these *Plasmodium*-associated compounds generally do not show significant differences between positive and negative cases could be explained by the fact the malaria-negative participants were not necessarily healthy controls. Participants visited the clinics because they experienced malaria symptoms and/or other ailments. Thus, these particular compounds previously reported to be associated with *Plasmodium*-infection may in fact be markers of a nonspecific infection. A case in point is nonanal, detected at a higher mass of 8.8–24.4 ng for positive case #17, which has been associated with TB infection, as have heptanal and octanal [7]. The possible non-specificity of these compounds is further supported by a study which has shown that compounds consistently found to be informative with regards to malaria status (e.g. hexanal, octanal and nonanal) have also been identified in the breath of lung and breast cancer patients, and that these compounds thus appear to be predictors of multiple diseases [14].

4. Conclusion

The cutaneous VOCs and SVOCs of malaria-negative and -positive individuals visiting two local clinics in Limpopo Province, South Africa, were collected using non-invasive PDMS sampling bands adhered to the surface of the human epidermis – providing a sample that is safer to handle and transport than traditional biofluids. These samplers are small, light-weight and portable, and easy to apply by trained non-medical personnel. A substantial benefit of the wearable epidermal sampler is that it is not restricted to, or reliant on, the blood stream as a means of detection, making it especially suitable to detect latent malaria cases. Detection of a promising differential putative marker of *Plasmodium*-infection, (E)-2-octen-1-ol, merits a follow-up study with a larger participant cohort.

The authors emphasise the need for cautious interpretation of results from cohorts that may include controls with comorbidities. Non-specificity should always be considered and potential markers of interest should not be assumed to be disease-specific.

Declaration of generative AI and AI-assisted technologies in the writing process

During the preparation of this work the authors used ChatGPT in order to generate an illustrative image from the corresponding author's own original photographs (available on request) of the cutaneous sampling procedure (Fig 1). After using this tool/service, the authors reviewed and edited the content as needed and take full responsibility for the content of the publication.

CRediT authorship contribution statement

Daniel T. Pretorius: Writing – review & editing, Writing – original draft, Methodology, Investigation, Formal analysis. **Egmont R. Rohwer:** Writing – review & editing, Resources, Conceptualization. **Yvette Naudé:** Writing – review & editing, Writing – original draft, Supervision, Resources, Formal analysis, Conceptualization.

Declaration of competing interest

The authors declare that they have no known competing financial interests or personal relationships that could have appeared to influence the work reported in this paper.

Acknowledgements

The authors are grateful to the late Prof Anton Stoltz (†2020), Department of Internal Medicine, Division of Infectious Diseases, University of Pretoria for funding; Dr Taneshka Kruger (UP ISMC), for her great support and guidance in the Vhembe district; the translators: Ms Salphinah and Ms Magidi (surnames unknown), Mpho Ramukosi; the staff of the Masisi and Madimbo clinics; Prof Veronica Ueckermann Head of Infectious Diseases, Department Internal Medicine, University of Pretoria and Steve Biko Academic Hospital for assistance with biological waste disposal; and Damian Vaz de Sousa for his assistance in compiling the heatmap using R© computational and statistical software.

Supplementary materials

Supplementary material associated with this article can be found, in the online version, at doi:10.1016/j.jcoa.2025.100233.

Data availability

Data will be made available on request.

References

[1] WHO. 2024. *World Malaria Report 2024*. https://www.who.int/teams/global-malaria-programme/reports/world-malaria-report-2024.
[2] Centres for Disease Control and Prevention, 2024. *Malaria*. https://www.cdc.gov/dpdx/malaria/index.html. Accessed 14/04/2025.
[3] D. Giraldo, S. Rankin-Turner, A. Corver, M. Tauxe, A.L. Gao, D.M. Jackson, L. Simubali, C. Book, J.C. Stevenson, P.E. Thuma, R.C. McCoy, A. Gordus, M. M. Mburu, E. Simulundu, C.J. McMeniman, Human scent guides mosquito thermotaxis and host selection under naturalistic conditions, Curr. Biol. 33 (2023) 1–16, https://doi.org/10.1016/j.cub.2023.04.050.
[4] A.Z. Bernaa and A.R. Odom John, Breath metabolites to diagnose infection clinical chemistry 68:1 (2022) 43–51. https://doi.org/10.1093/clinchem/hvab218.
[5] C.L. Schaber, N. Katta, L.B. Bollinger, M. Mwale, R. Mlotha-Mitole, I. Trehan, B. Raman, A.R. Odom John, Breathprinting reveals malaria-associated biomarkers and Mosquito attractants, JID 217 (2018) 1533–1560, https://doi.org/10.1093/infdis/jiy072.
[6] B. de Lacy Costello, A. Amann, H. Al-Kateb, C. Flynn, W. Filipiak, T. Khalid, D. Osborne, N.M. Ratcliffe, A review of the volatiles from the healthy human body, J Breath Res. 8 (2014) 14001, https://doi.org/10.1088/1752-7155/8/1/014001.
[7] P.C.K. Makhubela, E.R. Rohwer, Y. Naudé, Detection of tuberculosis-associated compounds from human skin by GCxGC-TOFMS, J. Chromatogr. B 1231 (2023) 123937, https://doi.org/10.1016/j.jchromb.2023.123937.
[8] J.A. Pickett, R.C. Smallegange, T. Bousema, J.G. Logan, A.O. Busula, M.A. Voets, A. Robinson, J.C. Caulfield, R.W. Sauerwein, N.O. Verhulst, K.B. Beshir, C. J. Sutherland, J.G. de Boer, M.A. Birkett, S.J. Powers, P. Winskill, J. Muwanguzi, D. K. Masiga, W. Takken, W.R. Mukabana, Plasmodium associated changes in human odour attract mosquitoes, Proc. Natl. Acad. Sci. 115 (18) (2018) 201721610.
[9] R. Lacroix, W.R. Mukabana, L.C. Gouagna, J.C. Koella, Malaria infection increases attractiveness of humans to mosquitoes, PloS Biol. 3 (9) (2005) e298, https://doi.org/10.1371/journal.pbio.0030298.
[10] A.O. Busula, T. Bousema, C.K. Mweresa, D. Masiga, J.G. Logan, R.W. Sauerwein, N. O. Verhulst, W. Takken, J.G. de Boer, Gametocytemia and attractiveness of Plasmodium falciparum-infected Kenyan children to Anopheles gambiae mosquitoes, J. Infect. Dis. 216 (3) (2017) 291–295, https://doi.org/10.1093/infdis/jix214.
[11] M. Kelly, C.-Y. Su, C. Schaber, J.R. Crowley, F.-F. Hsu, J.R. Carlson, A.R. Odom, Malaria parasites produce volatile mosquito attractants, mBio 6 (2) (2015), https://doi.org/10.1128/mBio.00235-15 e00235-15.
[12] C.M. de Moraes, N.M. Stanczyk, H.S. Betz, H. Pulido, D.G. Sim, A.F. Read, M. C. Mescher, Malaria-induced changes in host odors enhance mosquito attraction, PNAS 111 (30) (2014) 11079–11084, https://doi.org/10.1073/pnas.1405617111.
[13] A. Robinson, A.O. Busula, M.A. Voets, K.B. Beshir, J.C. Caulfield, S.J. Powers, N. O. Verhulst, P. Winskill, J. Muwanguzi, M.A. Birkett, R.C. Smallegange, D. K. Masiga, W.R. Mukabana, R.W. Sauerwein, C.J. Sutherland, T. Bousema, J. A. Pickett, W. Takken, J.G. Logan, J.G. de Boer, Plasmodium-associated changes in human odor attract mosquitoes, PNAS 115 (18) (2018) E4209–E4218, https://doi.org/10.1073/pnas.1721610115.
[14] H. Pulido, N.M. Stanczyk, C.M. de Moraes, M. Mescher, A unique volatile signature distinguishes malaria infection from other conditions that cause similar symptoms, Sci. Rep. 11 (2021) 139928, https://doi.org/10.1038/s41598-021-92962-x.
[15] E. Boudard, L. Fisson, N. Moumane, J. Dugay, J. Vial, D. Thiébaut, Study of sampling phases for body odor sampling prior to analysis by TD-GC×GC/ToFMS, Anal. Bioanal. Chem (2025) 1–14, https://doi.org/10.1007/s00216-025-05857-5.
[16] S. Rankin-Turner, C.J. McMeniman, A headspace collection chamber for whole body volatilomics, Analyst 147 (2022) 5210–5222, https://doi.org/10.1039/d2an01227h.
[17] K.T. Carrillo, N.S. Béziat, G. Cebrián-Torrejón, O. Gros, A.P. de la Mata, J. J. Harynuk, Metabolomic analysis of secondary metabolites from Caribbean crab gills using comprehensive two-dimensional gas chromatography - time-of-flight mass spectrometry —New inputs for a better understanding of symbiotic associations in crustaceans, J. Chromatogr. Open 2 (2022) 100069, https://doi.org/10.1016/j.jcoa.2022.100069.
[18] S. Ngxangxa, A.G.J. Tredoux, A. de Villiers, Comprehensive two-dimensional gas chromatography-high resolution mass spectrometry for the detailed qualitative analysis of old vine Chenin blanc wine volatiles and comparison with young vine Chenin blanc wines, J. Chromatogr. Open 5 (2024) 100116, https://doi.org/10.1016/j.jcoa.2024.100116.
[19] A.M. Muscalu, T. Górecki, Comprehensive two-dimensional gas chromatography in environmental analysis, Trends Anal. Chem. 106 (2018) 225–245, https://doi.org/10.1016/j.trac.2018.07.001.
[20] E.A. Higgins Keppler, C.L. Jenkins, T.J. Davis, H.D. Bean, Advances in the application of comprehensive two-dimensional gas chromatography in metabolomics, Trends Anal. Chem. 109 (2018) 275–286, https://doi.org/10.1016/j.trac.2018.10.015.
[21] M.S.S. Amaral, P.J. Marriott, The blossoming of technology for the analysis of complex aroma bouquets-A review on flavour and odorant multidimensional and comprehensive gas chromatography applications, Molecules 24 (2019) 2080, https://doi.org/10.3390/molecules24112080.
[22] M.S.S. Amaral, Y. Nolvachai, P.J. Marriott, Comprehensive two-dimensional gas chromatography advances in technology and applications: biennial update, Anal. Chem. 92 (2020) 85–104, https://doi.org/10.1021/acs.analchem.9b05412.
[23] S.L. Nam, A.P. de la Mata, R.P. Dias, J.J. Harynuk, Towards standardization of data normalization strategies to improve urinary metabolomics studies by GC×GC-TOFMS, Metabolites 10 (9) (2020) 376, https://doi.org/10.3390/metabo10090376.
[24] T.J. Trinklein, C.N. Cain, G.S. Ochoa, S. Schöneich, L. Mikaliunaite, R.E. Synovec, Recent advances in GC×GC and chemometrics to address emerging challenges in nontargeted analysis, Anal. Chem. 95 (2023) 264–286, https://doi.org/10.1021/acs.analchem.2c04235.
[25] M. Beccaria, C. Bobak, B. Maitshotlo, T.R. Mellors, G. Purcaro, F. Franchina, C. A. Rees, M. Nasir, A. Black, J.E. Hill, Exhaled human breath analysis in active pulmonary tuberculosis diagnostics by comprehensive gas chromatography-mass spectrometry and chemometric techniques, J.Breath Res. 5 (13) (2019) 016005, https://doi.org/10.1088/1752-7163/aae80e.
[26] R. Pesesse, P.-H. Stefanuto, F. Schleich, R. Louis, J.-F. Focant, Multimodal chemometric approach for the analysis of human exhaled breath in lung cancer patients by TD-GC × GC-TOFMS, J. Chromatogr. B 1114-1115 (2019) 146–153, https://doi.org/10.1016/j.jchromb.2019.01.029.
[27] A.P. Roodt, Y. Naudé, A. Stoltz, E. Rohwer, Human skin volatiles: passive sampling and GC×GC-ToFMS analysis as a tool to investigate the skin microbiome and interactions with anthropophilic mosquito disease vectors, J. Chromatogr. B 1097 (2018) 83–93, https://doi.org/10.1016/j.jchromb.2018.09.002.
[28] M. Wooding, E.R. Rohwer, Y. Naudé, Non-invasive sorptive extraction for the separation of human skin surface chemicals using comprehensive gas chromatography coupled to time-of-flight mass spectrometry: a mosquito-host biting site investigation, J. Sep. Sci. 43 (22) (2020) 4202–4215, https://doi.org/10.1002/jssc.202000522.
[29] M. Wooding E.R. Rohwer, Y. Naudé, Chemical profiling of the human skin surface for malaria vector control via a non-invasive sorptive sampler with GC×GC-TOFMS, Anal. Bioanal. Chem. 412 (23) (2020) 5759–5777, https://doi.org/10.1007/s00216-020-02799-y.
[30] M. Wooding, K. van Pletzen, Y. Naudé, Identifying skin surface chemicals as potential tuberculosis diagnostic biomarkers using ultra performance liquid chromatography-high resolution mass spectrometry, J. Chromatogr. Open (2025) 100204, https://doi.org/10.1016/j.jcoa.2025.100204.
[31] S. Triñanes, M.T. Pena, M.C. Casais, M.C. Mejuto, Development of a new Sorptive extraction method based on simultaneous direct and headspace sampling modes for the screening of polycyclic aromatic hydrocarbons in water samples, Talanta 132 (2015) 433–442, https://doi.org/10.1016/j.talanta.2014.09.044.
[32] H. van Den Dool, P.D. Kratz, A generalization of the retention index system including linear temperature programmed gas-liquid partition chromatography, J. Chromatogr. 11 (1963) 463–471, https://doi.org/10.1016/S0021-9673(01)80947-X.
[33] M. Kuhn, The caret package. http://topepo.github.io/caret/index.html, 2019 (accessed 23 November 2021).
[34] M. Kuhn, Building predictive models in R using the caret package, J. Stat. Softw. 28 (5) (2008) 1–26, https://doi.org/10.18637/jss.v028.i05.
[35] J. Zhang, Y. Zhang, L. Qiao, S. He, X. He, C. He, B. Chen, Y. Cao, Z.-B. He, AsOBP1 is required for host seeking in the malaria vector mosquito, Anopheles sinensis, J. Pest Sci. (2023) 1–26, https://doi.org/10.21203/rs.3.rs-2419325/v1.
[36] Z. Chen, F. Liu, N. Liu, Human odour coding in the yellow fever mosquito, Aedes Aegypti Sci. Rep. 9 (2019) 13336, https://doi.org/10.1038/s41598-019-49753-2.
[37] M.B. Markus, Malaria eradication and the hidden parasite reservoir, Trends Parasitol. 33 (7) (2017) 492–495, https://doi.org/10.1016/j.pt.2017.03.002.
[38] M.B. Markus, Biological concepts in recurrent plasmodium vivax malaria, Parasitology 145 (2018) 1765–1771, https://doi.org/10.1017/S003118201800032X.
[39] M. Wooding, T. Dodgen, E.R. Rohwer, Y. Naudé, Mass spectral studies on the human skin surface for mosquito vector control applications, J. Mass Spectrom. 56 (2) (2020) e4686, https://doi.org/10.1002/jms.4686.
[40] B.G.J. Knols, J.J.A. van Loon, A. Cork, R.D. Robinson, W. Adam, J. Meijerink, R. de Jong, W. Takken, Behavioural and electrophysiological responses of the female

malaria mosquito Anopheles gambiae (Diptera: culicidae) to Limburger cheese volatiles, B. Entomol. Res. 87 (2) (1997) 151–159, https://doi.org/10.1017/S0007485300027292.

[41] Y.T. Qiu, R.C. Smallegange, S. Hoppe, J.J.A. van Loon, E.-J. Bakker, W. Takken, Behavioural and electrophysiological responses of the malaria mosquito Anopheles gambiae Giles sensu stricto (Diptera: culicidae) to human skin emanations, Med, Vet, Entomol. 18 (4) (2004) 429–438, https://doi.org/10.1111/j.0269-283x.2004.00534.x.

[42] F. Kanda, E. Yagi, M. Fukuda, K. Nakajima, T. Ohta, O. Nakata, Elucidation of chemical compounds responsible for foot malodour, Brit. J. Dermatol. 122 (6) (1990) 771–776, https://doi.org/10.1111/j.1365-2133.1990.tb06265.x.